

Supporting Information for *Chemical Communications*

A Versatile Metal-Organic Framework for Carbon Dioxide Capture and Cooperative Catalysis

Jinhee Park,^a Jian-Rong Li,^a Ying-Pin Chen,^a Jiamei Yu,^b Andrey A. Yakovenko,^a Zhiyong U. Wang,^a Lin-Bing Sun,^a Perla B. Balbuena,^b and Hong-Cai Zhou^{a*}

^aDepartment of Chemistry, Texas A&M University, PO Box 30012, College Station, TX 77842-3012, USA

E-mail: zhou@mail.chem.tamu.edu

^bArtie McFerrin Department of Chemical Engineering, Texas A&M University, College Station, TX 77842, USA

1. Materials and Methods

2. Low-Pressure Sorption Measurements

3. Synthesis of PCN-124

4. X-ray Crystallography

5. PXRD, TGA, and IR, of PCN-124

6. Additional gas adsorption data

7. Calculation of heat of adsorption for H₂

8. Calculation of heat of adsorption for CO₂

9. Calculation of heat of adsorption for CH₄

10. Results of grand canonical Monte Carlo (GCMC) simulations on PCN-124

11. Tandem deacetalization-Knoevenagel condensation catalyzed by PCN-124

12. Refences

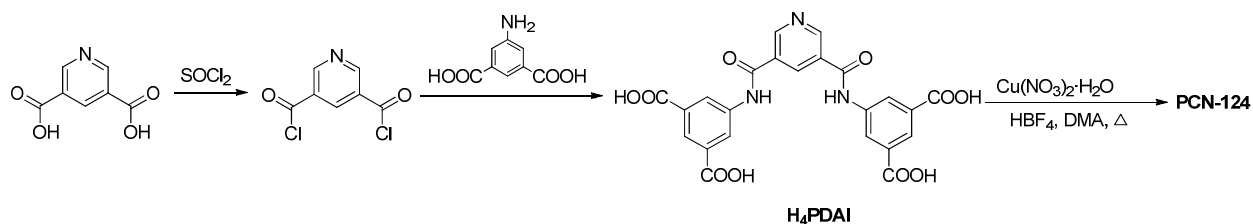
1. Materials and Methods

Commercially available reagents were used as received without further purification. ^1H nuclear magnetic resonance (NMR) data were recorded on a Mercury 300 MHz NMR spectrometer at the Center for Chemical Characterization and Analysis (CCCA), Department of Chemistry, Texas A&M University. Fourier transform infrared spectroscopy (FTIR) data were collected using a SHIMADZU IRAffinity-1 FTIR Spectrophotometer. Thermogravimetric analyses (TGA) were performed on a SHIMADZU TGA-50 Thermogravimetric Analyzer with a heating rate of $5\text{ }^\circ\text{C min}^{-1}$ under N_2 . Powder X-ray diffraction (PXRD) patterns were obtained on a BRUKER D8-Focus Bragg-Brentano X-ray Powder Diffractometer equipped with a Cu sealed tube ($\lambda = 1.54178$) at a scan rate of 0.5 s deg^{-1} , solid-state detector, and a routine power of 1400 W (40 kV, 35 mA). The simulated PXRD spectra were acquired by the diffraction-crystal module of the *Mercury* program based on the single crystal data. The program is available free of charge *via* internet at <http://www.iucr.org>.

2. Low-Pressure Sorption Measurements.

N_2 , H_2 , CO_2 and CH_4 isotherms of PCN-124 were measured up to 1 bar using a Micromeritics ASAP 2020 surface area and pore size analyzer. Pore size distribution data were calculated from the N_2 sorption isotherms based on DFT model in the Micromeritics ASAP2020 software package (assuming slit pore geometry). An as-synthesized sample was washed with and then immersed in fresh DMA for 24 h, and the extract was decanted. The sample was immersed in dry methanol for 48 h to remove the nonvolatile solvates such as DMA and water. After draining the methanol, fresh dichloromethane was subsequently added, and the sample was allowed to sit for 48 h. After the removal of dichloromethane, the sample was dried under a dynamic vacuum ($< 0.1\text{ mmHg}$) at room temperature overnight and then activated again by using the degassing function of the surface area analyzer for 10 h at $100\text{ }^\circ\text{C}$. A color change from green to deep purple-blue was observed, typical for Cu paddlewheel-based MOFs containing open Cu sites.

3. Synthesis of PCN-124



H₄PDAI: In a dried 250 mL round-bottomed flask was added anhydrous pyridine-3,5-dicarboxylic acid (2.0 g, 12.0 mmol) and thionyl chloride (40.0 mL, 0.55 mol). *N,N*-dimethylformamide (1.0 mL, 12.9 mmol) was carefully added dropwise, and the mixture was stirred and heated at 75 °C for 6 h under N₂ atmosphere. The excess SOCl₂ was removed under vacuum in a well-ventilated hood, quenched with ethanol and then water, and appropriately disposed. The residual pyridine-3,5-dicarbonyl chloride was used without further purification. Pyridine-3,5-dicarbonyl chloride (0.61 g, 3.0 mmol) was dissolved in anhydrous acetonitrile (20 mL) and added dropwise to a solution of 5-aminoisophthalic acid (1.27 g, 7.0 mmol) in acetonitrile (20 mL). The resulting mixture was stirred at room temperature for 24 h and then refluxed for 2 h. The precipitated white solid was isolated by filtration and washed with fresh acetonitrile (50 mL) followed by water (300 mL) to obtain 5,5'-((pyridine-3,5-dicarbonyl)bis(azanediyl))diisophthalic acid (**H₄PDAI**) (1.27 g, 86% yield for two steps) after overnight drying under vacuum (< 0.1 mmHg). ¹H-NMR (300 MHz, DMSO-*d*₆) δ 10.96 (s, 2 H), 9.33 (d, 2 H, *J*=2.0 Hz), 8.93 (t, 1 H, *J*=1.9 Hz), 8.69 (d, 4 H, *J*=1.5 Hz), 8.25 (t, 2H, *J*=1.5 Hz). IR (ν max): 3501, 3055, 2544, 1691, 1606, 1546, 1429, 1330, 1271, 1122, 908, 758, 684 cm⁻¹. See Figure S1. Mass spectrum: See Figure S2. Elemental analysis (% calc/found): C:55.9/53.1 N: 8.5/7.8 H: 3.0/3.8. IR: 3053, 1546, 1369, 1284, 1112, 908, 773, 734, 678, 601 cm⁻¹

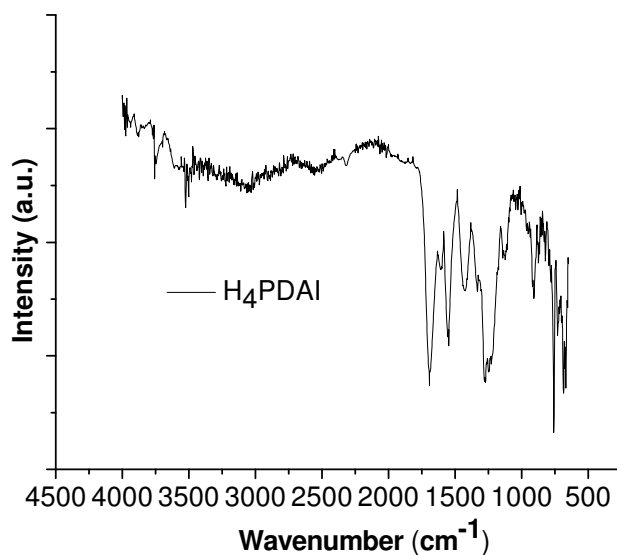


Figure S1. FT-IR spectrum of H₄PDAI.

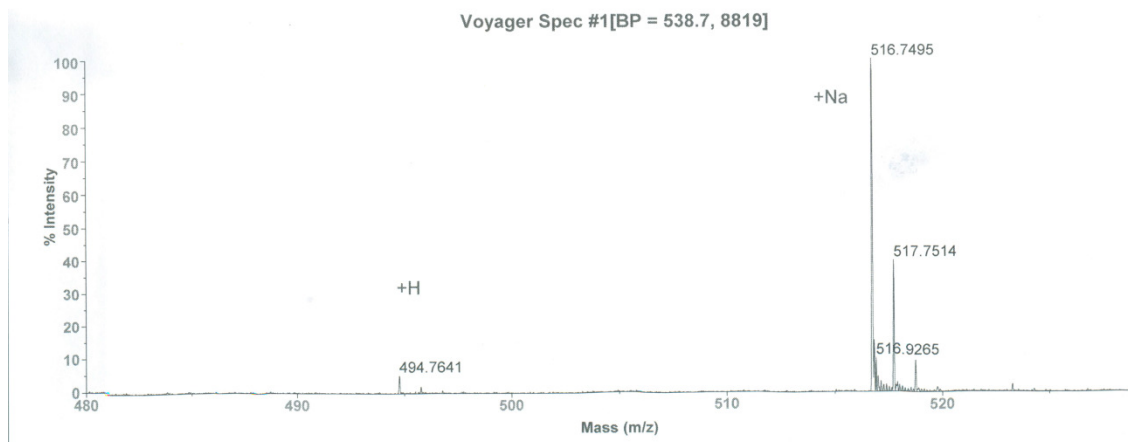


Figure S2. Mass spectrum of H₄PDAI. Ionization method: MALD, THAP matrix Used.

PCN-124: To a mixed solvent of dimethylacetamide (DMA, 12 mL) and water (3 mL) in a 20 mL scintillation vial was added **H₄PDAI** (40 mg, 0.081 mmol), Cu(NO₃)₂·2.5H₂O (120 mg, 0.016 mmol), and HBF₄ (48% in water, 30 drops). The vial was capped and allowed to sit in a 75 °C oven for 2 days. Green block crystals of **PCN-124** were collected (41 mg, 80 % yield) by filtration. IR: 3053, 1546, 1369, 1284, 1112, 908, 773, 734, 678, 601 cm⁻¹. See Figure S7. Elemental analysis (% calc/found): C: 43.6/42.8 N: 6.6/5.0 H: 1.7/4.2. PXRD and TGA of **PCN-124** are shown below.

4. X-ray Crystallography

For a single crystal analysis, a blue block crystal was taken directly from the mother liquor, transferred to oil and mounted into loop. Single crystal X-ray structure determination of PCN-124 was performed at 110 K on a Bruker APEX CCD diffractometer with MoK α radiation ($\lambda = 0.71703 \text{ \AA}$). Structures were solved by direct method and refined by full-matrix least-squares on F^2 using *SHELXTL*. Non-hydrogen atoms were refined with anisotropic displacement parameters during the final cycles. Organic hydrogen atoms were placed in calculated positions with isotropic displacement parameters set to $1.2 \times U_{\text{eq}}$ of the attached atom. The solvent molecules are highly disordered, and attempts to locate and refine the solvent peaks were unsuccessful. Contributions to scattering due to these solvent molecules were removed using the *SQUEEZE* routine of *PLATON*; structures were then refined again using the data generated.

Crystal data for PCN-124: $\text{C}_{23}\text{H}_{11}\text{N}_3\text{O}_{11}\text{Cu}_2$, green block, cubic, space group $Im\bar{3}m$ (No. 229), $a = 30.585 (12) \text{ \AA}$, $V = 28611 (19) \text{ \AA}^3$, $Z = 24$, $D_c = 0.881 \text{ g/cm}^3$, $F_{000} = 11492$, Mo K α radiation = 0.71073 \AA , $T = 110(2) \text{ K}$, $\theta_{\text{max}} = 28.70^\circ$, 180466 reflections collected, 3484 unique ($R_{\text{int}} = 0.1186$). Final $GOOF = 1.029$, $RI = 0.0914$, $wR2 = 0.1966$, R indices based on 2829 reflections with $I > 2\sigma(I)$ (refinement on F^2). The CIF file can be obtained free of charge from the Cambridge Crystallographic Data Centre via www.ccdc.cam.ac.uk/data_request/cif (CCDC 858820).

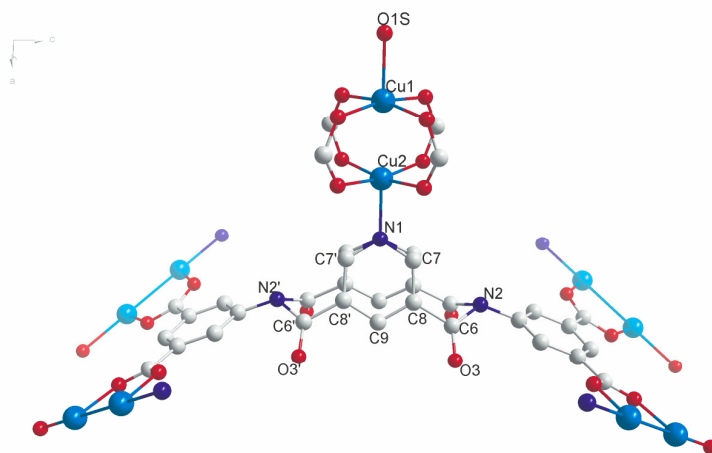


Figure S3. Fragmental clusters and the atomic labels in PCN-124. Cu atoms are shown in cyan, O atoms in red, N atoms in blue, C atoms in grey.

In the process of structure refinement of the PCN-124, it was found that the ligand oriented in a special position and was lying on the mirror plane. At the same time, atoms in central pyridine ring (N1-C7-C8-C9-C8'-C7') and carboxylate side chain (O6-C3) have enlarged displacement ellipsoids oriented perpendicular to the mirror plane. That was attributed to the disorder of the central ligand fragment by two positions about the mirror plane. Such disorder was modeled successfully; it was refined with the help of FLAT restrain on atoms N1 C7 C8 C9, as well as rigid bond restraints for anisotropic displacement parameters. The relative occupancies for the disordered components were fixed to be 50%. The dihedral angle between the average planes of the disordered parts is found to be 13.7°, which probably corresponds to two different orientations of the ligand molecule present in the framework.

With $Z = 24$ in a cubic high-symmetry space group there is space-group imposed symmetry in this structure. Cu1, Cu2, N1 and O1S lie at sites with $m.m2$ -symmetry. C9 and H9A lie at sites with $m..$ -symmetry. N2, C5, C2, H2B, H7A lie at sites with $..m$ -symmetry. O1, O2, C1, C3, C4, H4A, O3, C6, C7, C8, H2A lie at general positions.

To justify the selection of $Im\bar{3}m$ symmetry, intensity data was integrated in triclinic crystal system. After introducing data to XPREP, it has shown that the $R(\text{sym})$ for Cubic I lattice is 0.22 which is similar to other Bravais lattices, excluding Monoclinic C ($R(\text{sym})=0.165$) and Triclinic ($R(\text{sym})=0.000$). Hence, the structure was resolved in Monoclinic C $2/m$ and $C2$ space groups. However, similar disorder appears for the ligand as observed in $Im\bar{3}m$ case. Hence, it indicates that higher symmetry of Bravais lattice should be applied.

In case of Cubic I crystal system, XPREP lists several space groups and $I23$ (CFOM=27.86), $Im\bar{3}m$ (CFOM=17.58), $I\bar{4}3m$ (CFOM=17.39) as the best candidates with lowest CFOM factor. After solving the structure in these groups, the same disorder of the ligand is present. Also after checking the structure in PLATON addsym unit, it shows that the correct space group should be $Im\bar{3}m$. $Im\bar{3}m$ is the best space group for this structure which correctly describes symmetry of the structure.

A mixed solvent of dimethylacetamide (DMA, $\text{CH}_3\text{C}(\text{O})\text{N}(\text{CH}_3)_2$, 12 mL) and water (3 mL) were used in the synthesis process. Therefore, electron density of these both solvents was removed by SQUEEZE process. However, we cannot exactly calculate the amount of each component. Assuming that ratio of water and DMA inside the pores to be 1:1, which is the same as in solution. Since one DMA molecule contains 48 electrons and one water molecule contains 10 electrons, then we can calculate $3908/(48+10) = 67.37$, hence we removed approximately 67 DMA molecules and 67 water molecules from the unit cell. Since $Z=24$, we have approximately 3 DMA molecules and 3 water molecules in the unit. However, PCN-124 is synthesized in solvothermal conditions, hence DMA may decompose, and the products of decomposition may be in the pores instead of DMA. In this case, we want to say that determination of the MOF pores content after reaction is very complicated task and not the point of this particular work. Therefore, we have corrected the $F(000)$ value, but parameters such as overall formula, formula weight, density, etc. in our opinion cannot be corrected for the reasons explained above.

Table S1. PCN-124 crystal information

Compound	PCN-124
Formula	C ₂₃ H ₁₁ N ₃ O ₁₁ Cu ₂
MW [g·mol ⁻¹]	632.43
Crystal system	Cubic
Space group	<i>Im</i> $\bar{3}$ <i>m</i>
<i>a</i> [Å]	30.585 (12)
<i>b</i> [Å]	30.585 (12)
<i>c</i> [Å]	30.585 (12)
α [deg]	90.00
β [deg]	90.00
γ [deg]	90.00
<i>V</i> [Å ³]	28611 (19)
<i>T</i> [K]	110 (2)
<i>Z</i>	24
<i>D</i> _{calc} [g·cm ⁻³]	0.881
μ [mm ⁻¹]	0.927
Min/max transmission	0.9380/0.9049
θ_{\max} [deg]	28.70
Measured reflections	180466
Unique reflections	3484
Reflections [<i>F</i> ₀ > 4 σ (<i>F</i> ₀)]	2829
Parameter	93
<i>R</i> _{int}	0.1186
<i>R</i> ₁ [<i>F</i> ₀ > 4 σ (<i>F</i> ₀)]	0.0914
<i>wR</i> ₂ [all data]	0.1966
GOF	1.029

5. PXRD, TGA, and IR, of PCN-124

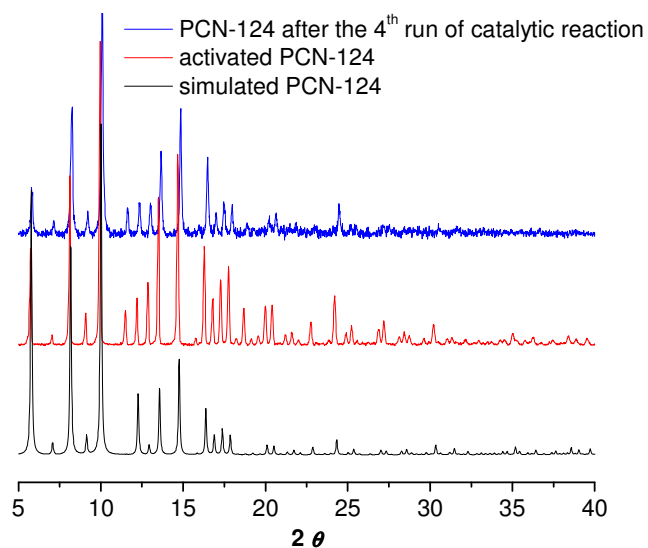


Figure S4. PXRD of simulated, activated PCN-124 and PCN-124 after the 4th run of catalytic reaction.

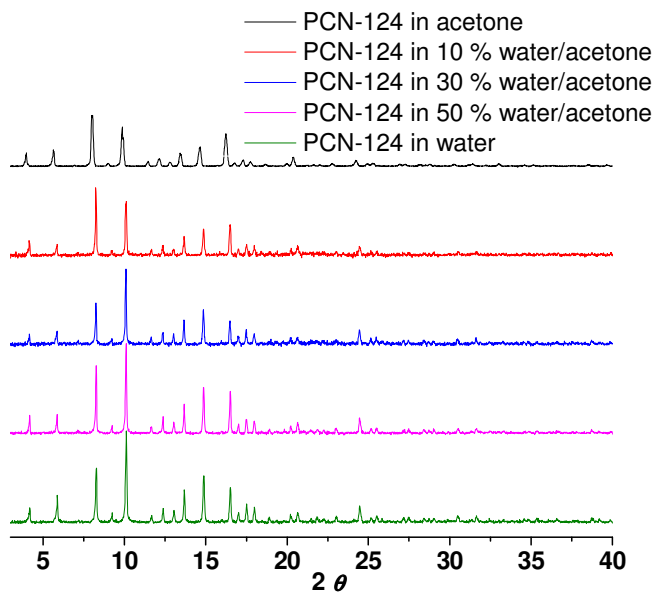


Figure S5. PXRD of PCN-124 in acetone, 10 % water/acetone, 30% water/acetone, 50 % water/acetone and 100% water for 2 days. Crystallinity of PCN-124 was maintained even in water for 2 days.

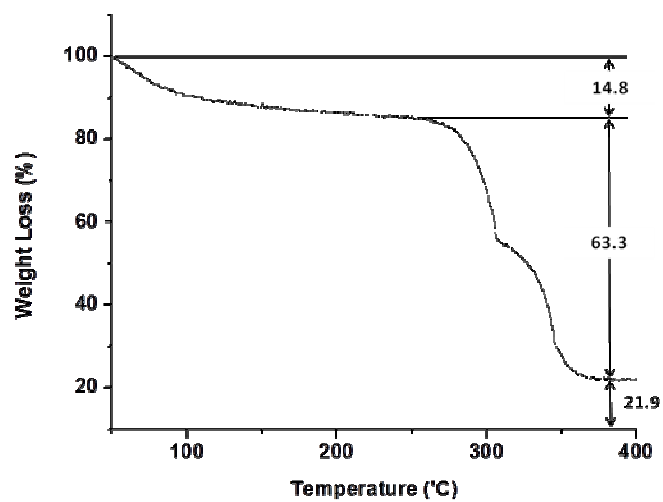


Figure S6. TGA of PCN-124.

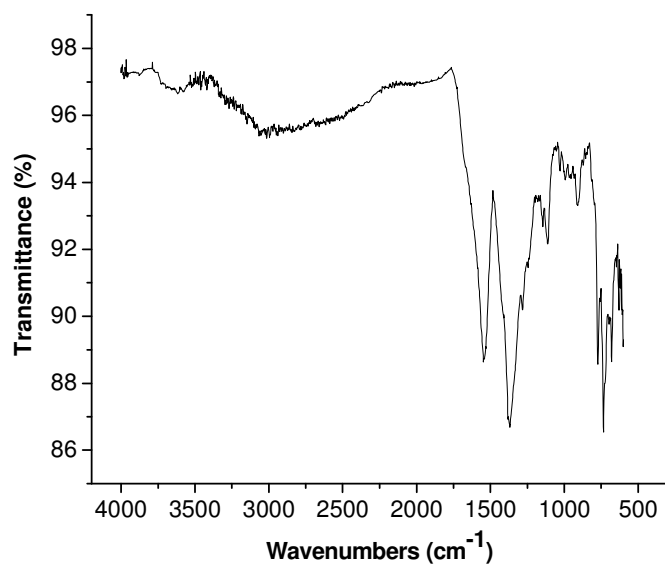


Figure S7. FT-IR of activated PCN-124.

6. Additional gas adsorption data

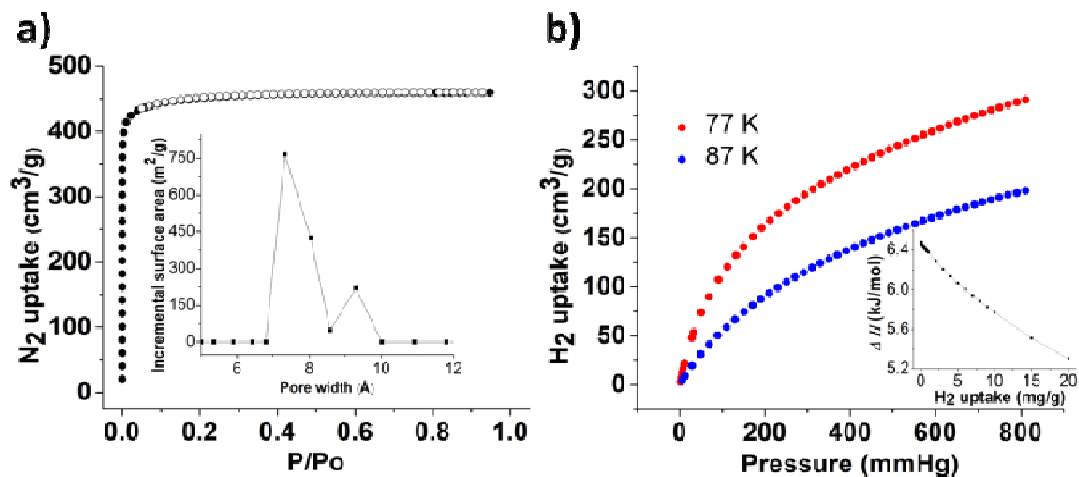


Figure S8. (a) N₂ adsorption isotherm of **PCN-124** and its pore size distribution (inset). (b) H₂ adsorption isotherm of **PCN-124** at 77 K and 87 K and the heat of H₂ adsorption (inset).

PCN-124 was found to have high uptake capacity for H₂, a favorable feature for clean energy-related gas adsorptions. The H₂ uptake at 77 K and 87 K at 800 mmHg was 2.5 wt% and 1.7 wt% (Figure S8 (b)), respectively, which are among the highest H₂ storage capacity of MOFs at atmospheric pressure.¹ The high capacity in the low pressure region can be mainly attributed to the small micropores of **PCN-124** as well as strong interactions between H₂ and unsaturated Cu²⁺ sites and the polar functional groups of the ligand, here, amide.² The isosteric heat of adsorption at zero H₂ loading was calculated to be 6.5 kJ/mol using a virial-type adsorption isotherm equation.³

7. Calculation of heat of adsorption for H₂

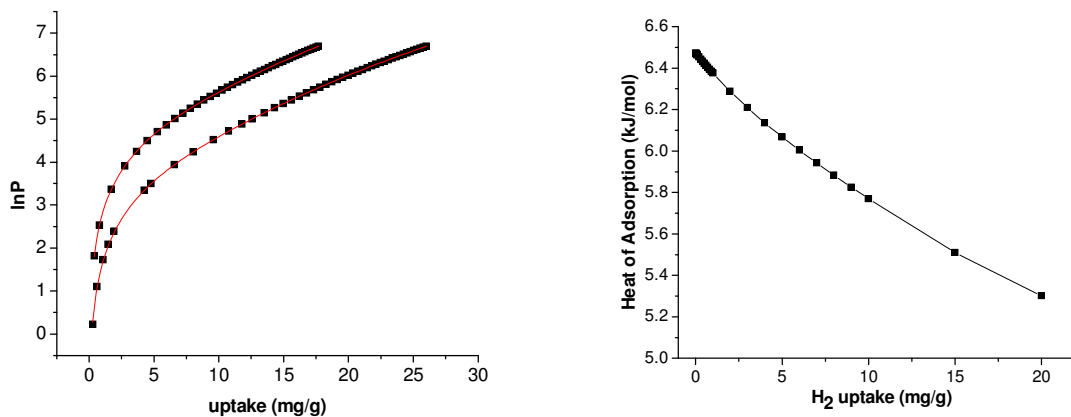


Figure S9. Nonlinear curve fitting of H₂ adsorption isotherms at 77 K and 87 K and heat of adsorption for H₂ in PCN-124.

$$y = \ln(x) + 1/k * (a_0 + a_1 * x + a_2 * x^2 + a_3 * x^3 + a_4 * x^4 + a_5 * x^5) + (b_0 + b_1 * x + b_2 * x^2)$$

Reduced Chi-Sqr		7.67E-05
Adj. R-Square		0.99996
	Value	Standard Error
a0*	-778.60453	4.58541
a1*	12.4354	1.08768
a2*	-0.74959	0.09461
a3*	0.05118	0.00937
a4*	-0.00183	3.94E-04
a5*	2.36E-05	5.95E-06
b0*	11.63244	0.05737
b1*	-0.05012	0.01379
b2*	0.0017	7.02E-04

8. Calculation of heat of adsorption for CO₂

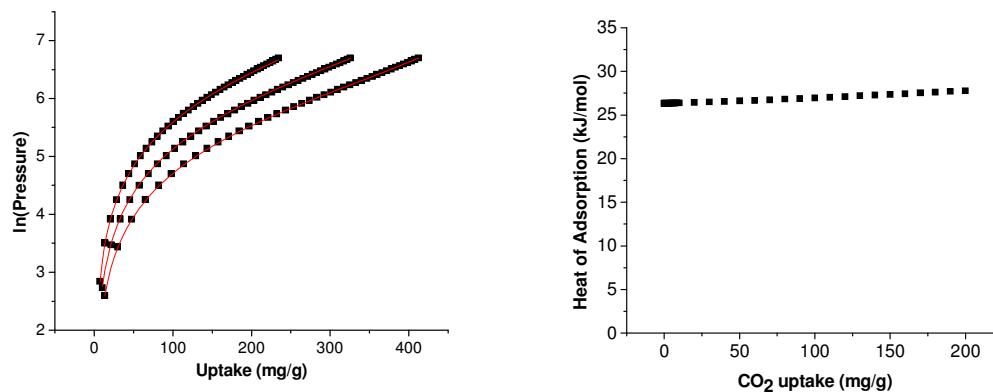


Figure S10. Nonlinear curve fitting of CO₂ adsorption isotherms at 273 K, 283 K and 295 K and CO₂ heat of adsorption for PCN-124.

$$y = \ln(x) + 1/k * (a_0 + a_1 * x + a_2 * x^2 + a_3 * x^3 + a_4 * x^4 + a_5 * x^5) + (b_0 + b_1 * x + b_2 * x^2)$$

Reduced Chi-Sqr		1.55E-04
Adj. R-Square		0.99982
	Value	Standard Error
a0*	-3166.53078	37.74311
a1*	-0.56695	0.52155
a2*	-0.00214	0.0021
a3*	2.67E-06	9.96E-06
a4*	-8.40E-09	2.65E-08
a5*	1.18E-11	2.54E-11
b0*	11.59251	0.13176
b1*	0.00311	0.00182
b2*	7.53E-06	5.70E-06

9. Calculation of heat of adsorption for CH₄

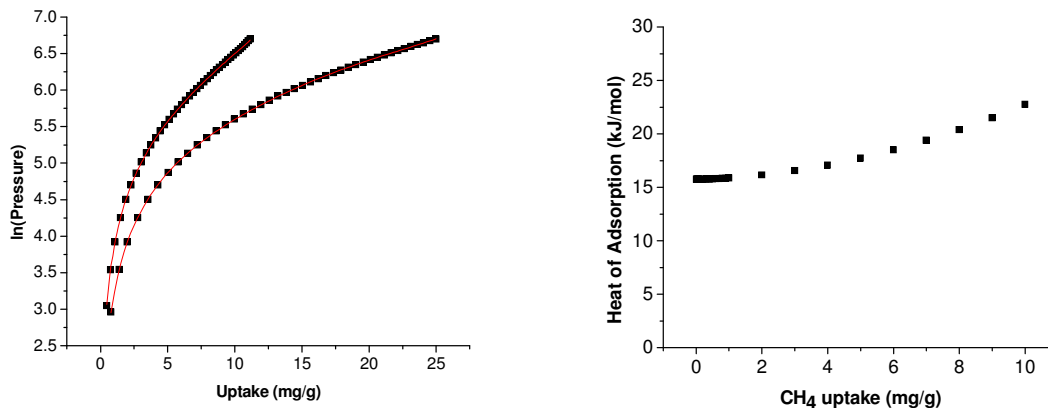


Figure S11. Nonlinear curve fitting of CH₄ adsorption isotherms at 273 K and 295 K and CH₄ heat of adsorption for PCN-124.

$$y = \ln(x) + 1/k * (a_0 + a_1 * x + a_2 * x^2 + a_3 * x^3 + a_4 * x^4 + a_5 * x^5) + (b_0 + b_1 * x + b_2 * x^2)$$

Reduced Chi-Sqr		2.28E-05
Adj. R-Square		0.99997
	Value	Standard Error
a0*	-1892.78116	14.44931
a1*	-8.10067	5.35599
a2*	-8.59266	0.50501
a3*	0.14861	0.02212
a4*	-0.00604	9.52E-04
a5*	8.92E-05	1.49E-05
b0*	10.10813	0.04909
b1*	0.06368	0.01738
b2*	0.02571	0.00132

10. Results of grand canonical Monte Carlo (GCMC) simulations on PCN-124

In pursuing the simulation of gas adsorptions in PCN-124, the partial charges for all the atoms of the framework were firstly calculated using DFT. The fragmental clusters used for charge calculation are shown in Figure S12. The terminations are all connected with organic linkers, and saturated with $-\text{CH}_3$ groups as done in previous published papers.⁴ DFT calculation based on CHELPG⁵ using B3LYP functional were carried out to compute the atomic partial charges. The basis set used for heavy atoms Cu is LANL2DZ; and 6-31G* was employed for the rest of the atoms.

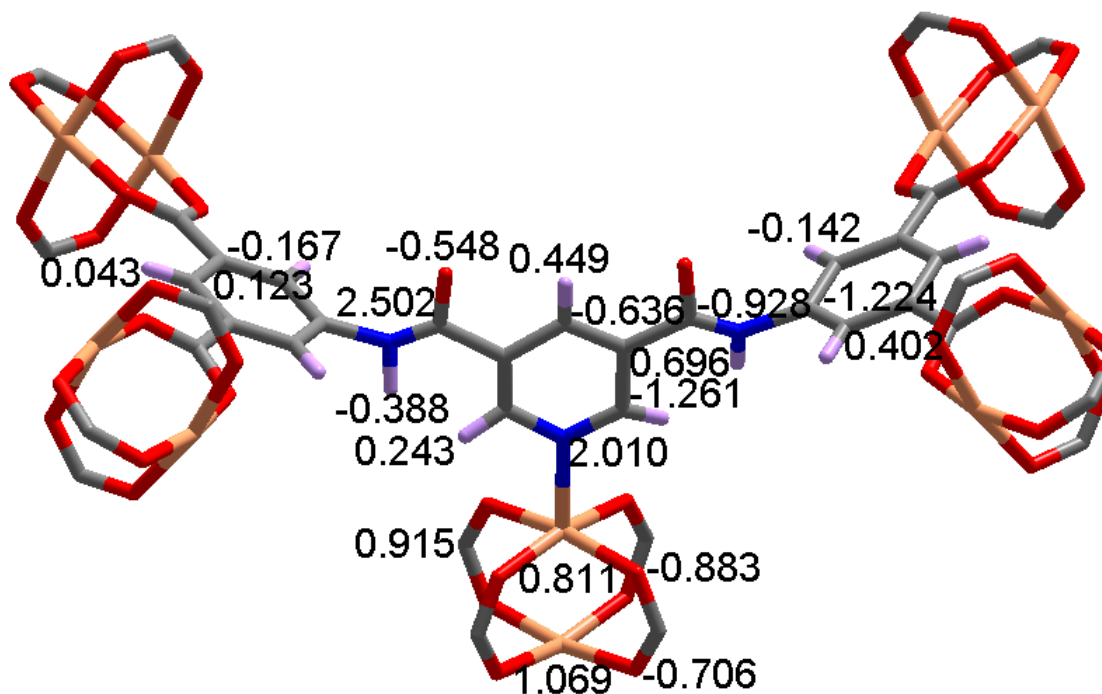


Figure S12. Fragmental clusters and the atomic partial charges in PCN-124. Color scheme for Cu atoms, tan ; O atoms, red; C atoms, grey; N atoms, blue; and H atoms, lavender.

Grand Canonical Monte Carlo (GCMC) simulations⁶ using MUSIC code⁷ were employed to calculate the adsorption of CO_2 and CH_4 in the PCN-124. PCN-124 frameworks were treated as rigid frameworks. A cutoff radius of 12.8 Å was applied to the LJ potential and Ewald summations were used to evaluate long range effects of the electrostatic interactions.⁸ Each

GCMC simulation consisted of 1×10^7 steps to guarantee equilibrium and 1×10^7 production steps.

CO₂ was represented as a rigid linear triatomic molecule with one charged Lennard-Jones (LJ) interaction site located at each atom. The LJ potential parameters are $\sigma_{OO} = 0.305$ nm and $\epsilon_{OO}/k_B = 79.0$ K for O-O interactions and $\sigma_{CC} = 0.280$ nm and $\epsilon_{CC}/k_B = 27.0$ K for C-C interactions between CO₂ molecules with a C-O bond length of 0.116 nm. Partial point charges are centered at each LJ site with $q_O = -0.35e$ and $q_C = 0.70e$. CH₄ was modeled as a single LJ interaction sites with $\sigma_{CH_4} = 0.373$ nm and $\epsilon/k_B = 148$ K. The LJ potential parameters for the framework atoms in PCN-124 were taken from UFF⁹ force field, as shown in Table S2. Lorentz-Berthelot mixing rules were employed to calculate the pair site-site interactions among the framework and each gas species.

Table S2. Potential parameters for the atoms in the framework of PCN-124.

atoms	σ (nm)	ϵ/v_B (K)
O	0.311	30.19
C	0.343	52.84
H	0.257	22.14
N	0.326	34.72
Cu	0.312	2.52

To understand the adsorption behavior of CO₂ in **PCN-124** at the molecular level, snapshots of the structures with adsorbed gas molecules at 0.2, 0.5 and 1 atm were analyzed (Figure S13). It was found that at low pressure, the CO₂ molecules prefer to be located in the pores containing both unsaturated Cu²⁺ sites and the amide groups. The pores only having unsaturated Cu²⁺ sites are less occupied by CO₂ molecules than the ones having both sites. The results indicate that the amide group is one of the primary CO₂ binding sites in **PCN-124** and corroborate the success of our design.

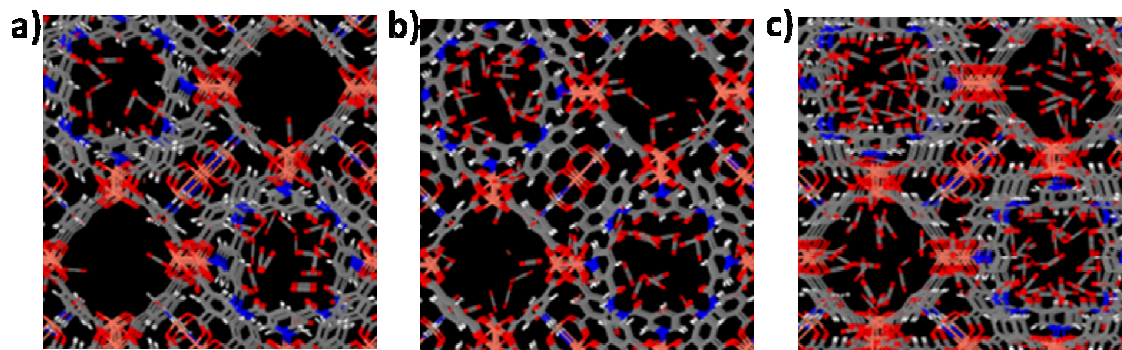


Figure S13. Snapshots of the structures with adsorbed CO₂ molecules at 295 K and a) 0.2 atm, b) 0.5 and c) 1.0 atm.

11. Tandem deacetalization-Knoevenagel condensation catalyzed by PCN-124:

Benzaldehyde dimethylacetal (0.30 g, 2.0 mmol) and malononitrile (0.14 g, 2.1 mmol) in DMSO-*d*₆ (3 mL) were stirred for 10 min. **PCN-124** (6 mg, 0.01 mmol, 0.5 mol%) was then added and stirring was continued at 50 °C for 12 h. To eliminate the effect of residual solvents in **PCN-124** from its preparation, the fully solvent-exchanged and activated sample was used. For the acidic and basic control experiments, *p*-Toluenesulfonic acid (95 mg, 0.5 mmol) and ethylenediamine (20 μL) were added to the reaction mixture respectively. These control experiments were also performed at the same temperature for the same duration. The progress of the reaction was directly monitored by ¹H NMR. **PCN-124** was recovered by centrifugal separation, washed with DMSO, and recycled. Due to hygroscopic DMSO, water was not added into the reaction mixture.

The yields were calculated by integration of benzylic protons at the end of the reaction. (Starting **1**: around 5.3 ppm, Product **2**: around 10.0 ppm, Product **3**: around 8.5 ppm)

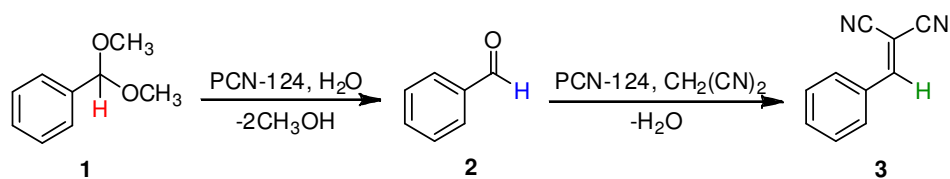


Table S3. ^1H NMR integration of the characteristic benzylic protons (Starting **1**: around 5.3 ppm, Product **2**: around 10.0 ppm, Product **3**: around 8.5 ppm).

	Starting 1	Product 2	Product 3
1	n/a	n/a	1
2	n/a	1	28.65
3	0.01	1	11.39
4	0.13	1	29.29
Acidic Control Rxn.	0.04	1	0.19
Basic Control Rxn.	1	0	0

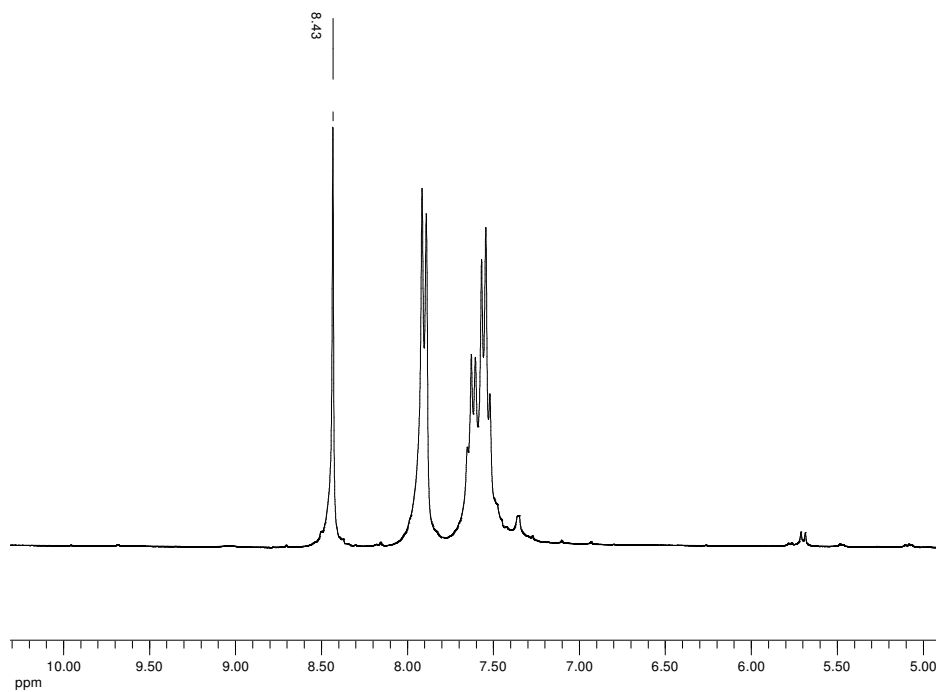


Figure S14. ^1H NMR spectrum of a solution after the first Deacetalization-Knoevenagel condensation catalyzed by PCN-124.

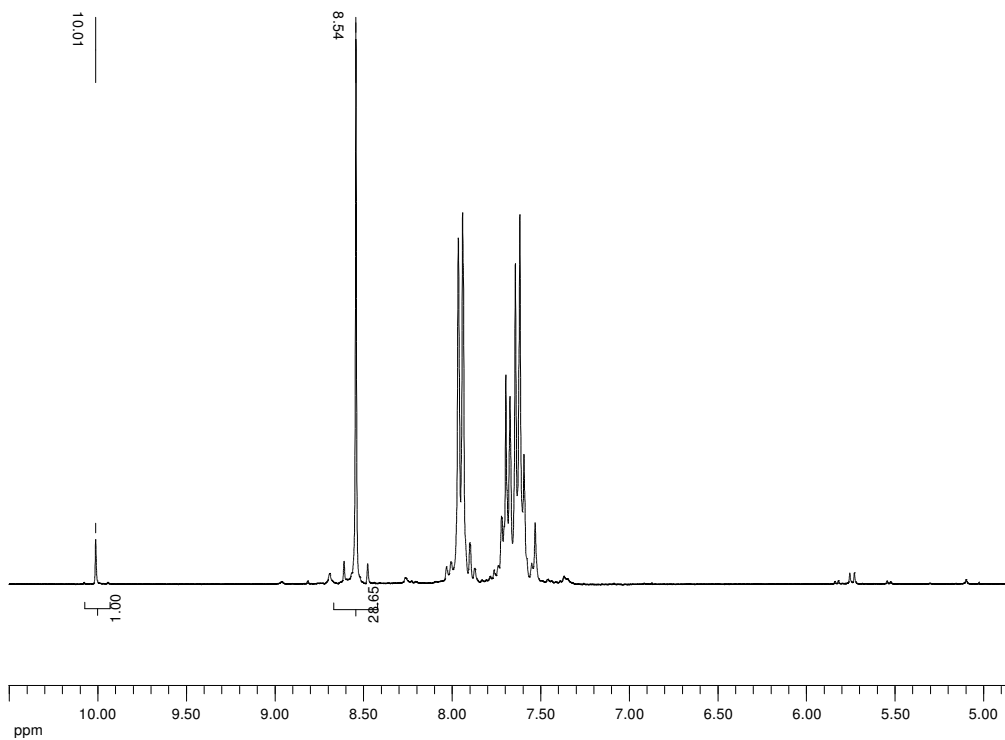


Figure S15. ¹H NMR spectrum of a solution after the second Deacetalization-Knoevenagel condensation catalyzed by PCN-124.

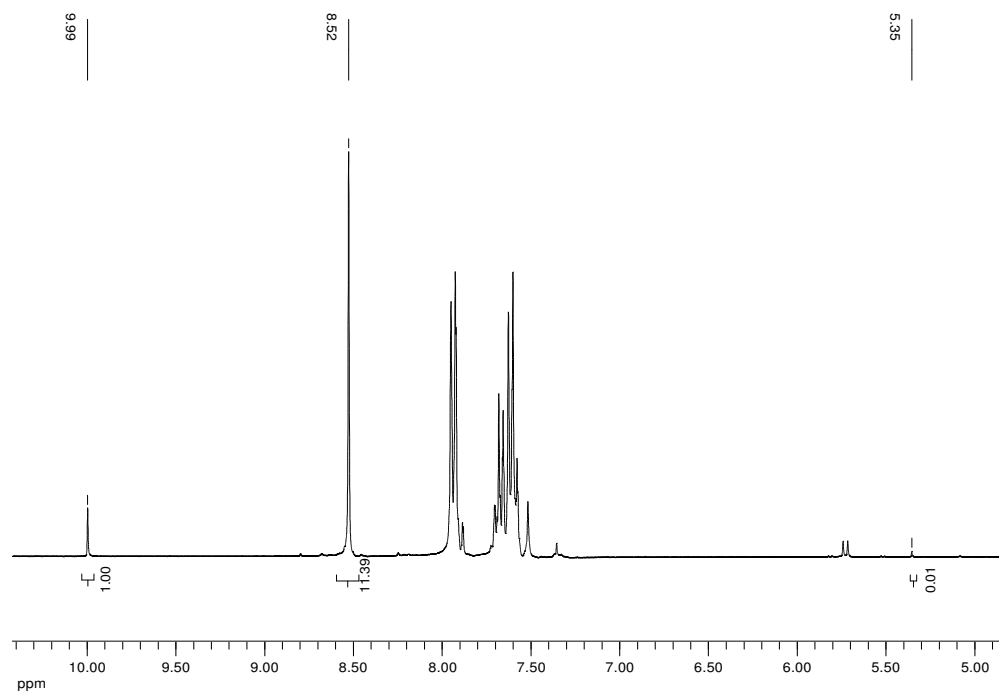


Figure S16. ^1H NMR spectrum of a solution after the third Deacetalization-Knoevenagel condensation catalyzed by PCN-124.

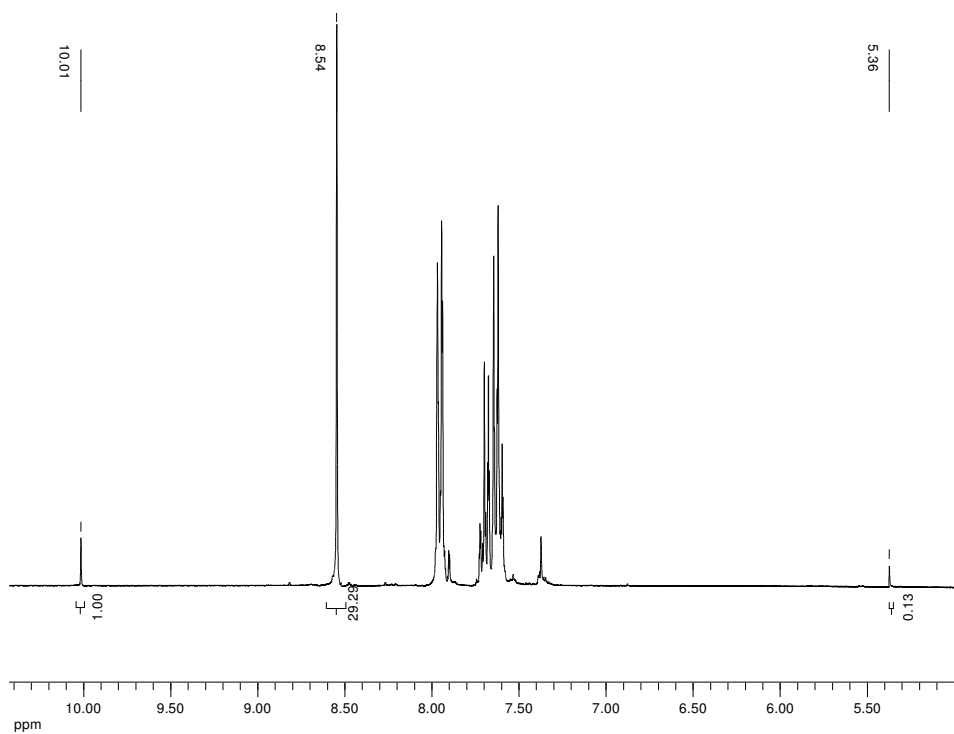


Figure S17. ¹H NMR spectrum of a solution after the fourth Deacetalization-Knoevenagel condensation catalyzed by PCN-124.

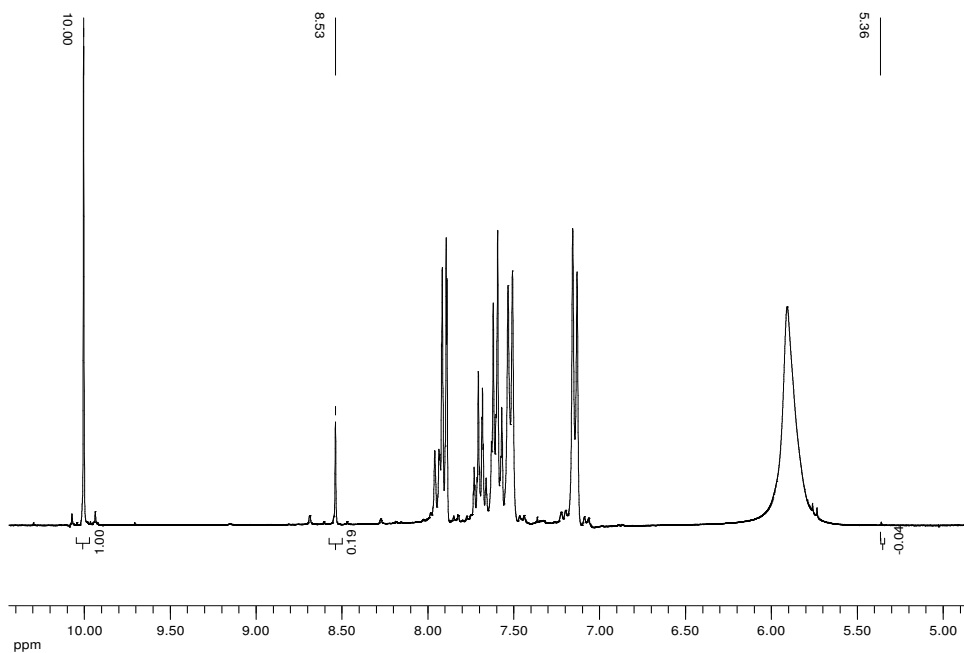


Figure S18. ¹H NMR spectrum of a solution after the Deacetalization-Knoevenagel condensation in acidic control reaction.

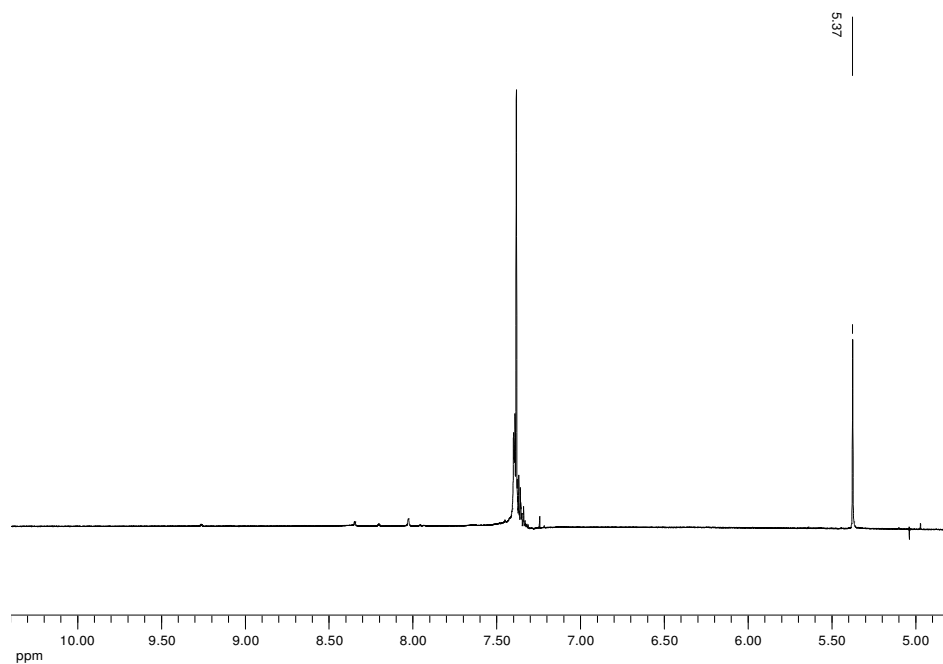


Figure S19. ¹H NMR spectrum of a solution after the Deacetalization-Knoevenagel condensation in basic control reaction.

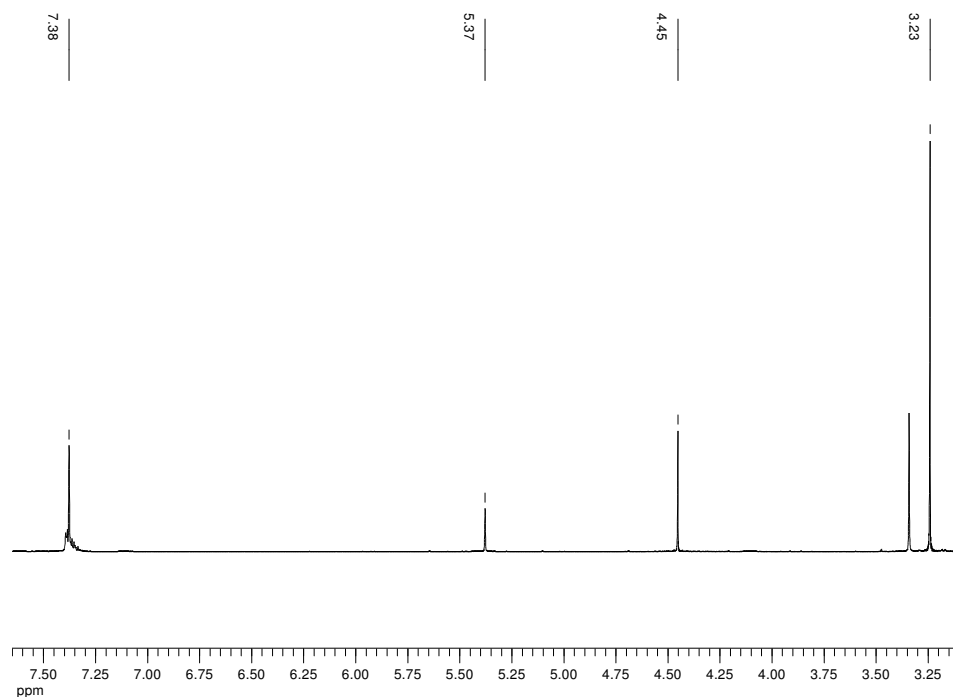


Figure S20. ¹H NMR spectra of a mixture of malononitrile and benzaldehyde dimethylacetal without catalyst.

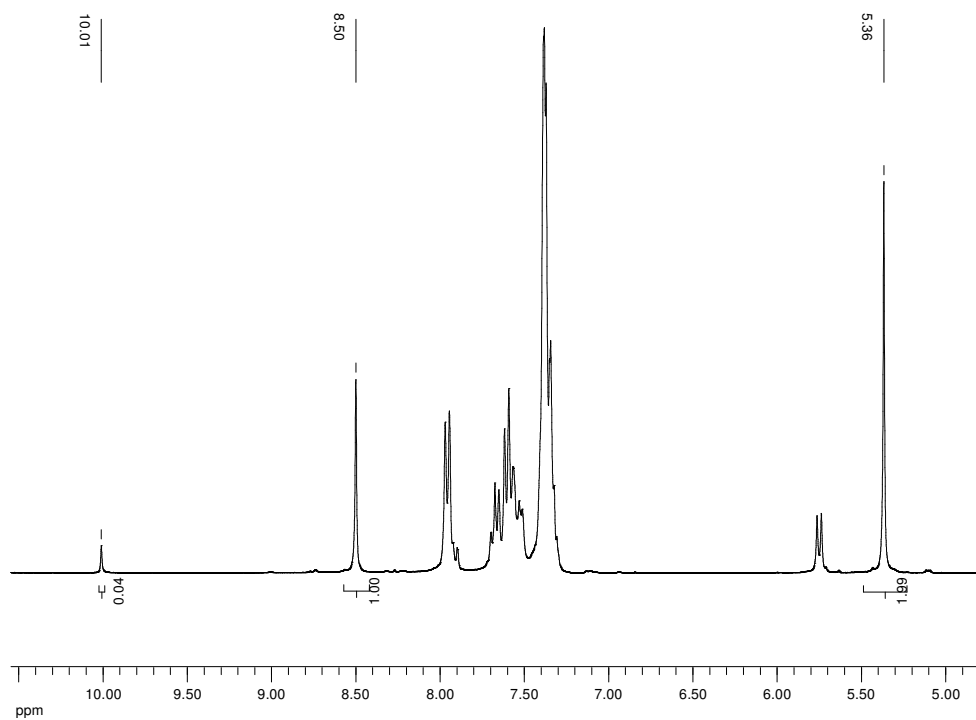


Figure S21. ¹H NMR spectrum of a solution at 4 h after the Deacetalization-Knoevenagel condensation catalyzed by PCN-124.

12. References

1. (a) X. Lin, I. Telepeni, A. J. Blake, A. Dailly, C. M. Brown, J. M. Simmons, M. Zoppi, G. S. Walker, K. M. Thomas, T. J. Mays, P. Hubberstey, N. R. Champness and M. Schröder, *J. Am. Chem. Soc.*, 2009, **131**, 2159; (b) W. Lu, D. Yuan, T. A. Makal, J.-R. Li and H.-C. Zhou, *Angew. Chem. Int. Ed.*, 2012, **51**, 1580.
2. (a) X.-S. Wang, S. Ma, P. M. Forster, D. Yuan, J. Eckert, J. J. López, B. J. Murphy, J. B. Parise and H.-C. Zhou, *Angew. Chem. Int. Ed.*, 2008, **47**, 7263; (b) R. Luebke, J. F. Eubank, A. J. Cairns, Y. Belmabkhout, L. Wojtas and M. Eddaoudi, *Chem. Commun.*, 2012; (c) D. Lässig, J. Lincke, J. Moellmer, C. Reichenbach, A. Moeller, R. Gläser, G. Kalies, K. A. Cychosz, M. Thommes, R. Staudt and H. Krautscheid, *Angew. Chem. Int. Ed.*, 2011, **50**, 10344.
3. (a) J. L. C. Rowsell and O. M. Yaghi, *J. Am. Chem. Soc.*, 2006, **128**, 1304; (b) A. Ansón, J. Jagiello, J. B. Parra, M. L. Sanjuán, A. M. Benito, W. K. Maser and M. T. Martínez, *J. Phys. Chem. B*, 2004, **108**, 15820; (c) L. Czepirski and J. JagieŁŁo, *Chem. Eng. Sci.*, 1989, **44**, 797.
4. (a) Q. Yang and C. Zhong, *J. Phys. Chem. B*, 2006, **110**, 17776; (b) C. Zheng, D. Liu, Q. Yang, C. Zhong and J. Mi, *Industrial & Engineering Chemistry Research*, 2009, **48**, 10479.
5. M. M. Francl, C. Carey, L. E. Chirlian and D. M. Gange, *J. Comput. Chem.*, 1996, **17**, 367.
6. M. P. Allen and D. J. Tildesley, *J. Computer Simulation of Liquides*, Oxford University Press, Oxford, 1987.
7. A. Gupta, S. Chempath, M. J. Sanborn, L. A. Clark and R. Q. Snurr, *Mol. Simulat.*, 2003, **29**, 29.
8. S. W. Deleeuw, J. W. Perram and E. R. Smith, *Proceedings of the Royal Society of London Series a-Mathematical Physical and Engineering Sciences* 1980, **373**, 27.
9. A. K. Rappe, C. J. Casewit, K. S. Colwell, W. A. Goddard and W. M. Skiff, *J. Am. Chem. Soc.*, 1992, **114**, 10024.